

# SDSSJ140228.22+632133.3: A NEW SPECTROSCOPICALLY SELECTED GRAVITATIONAL LENS<sup>1,2</sup>

ADAM S. BOLTON<sup>3</sup>, SCOTT BURLES<sup>3</sup>, LÉON V. E. KOOPMANS<sup>4</sup>, TOMMASO TREU<sup>5,7</sup>, AND LEONIDAS A. MOUSTAKAS<sup>6</sup>

*Draft version November 18, 2018*

## ABSTRACT

We present Gemini integral-field unit (IFU) spectroscopy and *Hubble Space Telescope* (HST) F435W- and F814W-band images of a newly discovered four-image gravitational lens, SDSSJ140228.22+632133.3 (hereafter SDSSJ1402). The system was identified as one of 49 gravitational-lens candidates in the luminous red galaxy sample of the Sloan Digital Sky Survey, based on higher-redshift emission lines in the spectra of the lower-redshift galaxies. We are imaging the most promising lens candidates with HST as part of a Snapshot program designed to expand the sample of known gravitational lenses amenable to detailed photometric, lensing and dynamical studies; SDSSJ1402 was the first of our targets to be observed with the ACS-WFC on board HST. The lens is a smooth elliptical galaxy at a redshift of  $z_l = 0.2046 \pm 0.0001$  with a Sloan  $r$ -band magnitude of  $17.00 \pm 0.05$  and a stellar velocity dispersion of  $267 \pm 17 \text{ km s}^{-1}$ , obtained from its SDSS spectrum. Multiple emission lines place the quadruply-imaged source at a redshift of  $z_s = 0.4814 \pm 0.0001$ . The best-fitting singular isothermal ellipsoid lens model gives an Einstein radius  $b = 1''.35 \pm 0''.05$  (or  $[4.9 \pm 0.2]h_{65}^{-1} \text{ kpc}$ ), corresponding to a total mass of  $(30.9 \pm 2.3) \times 10^{10} h_{65}^{-1} M_\odot$  within the critical curve. In combination with HST photometry this gives a rest-frame  $B$ -band mass-to-light ratio of  $(8.1 \pm 0.7)h_{65}$  times solar within the same region. The lens model predicts a luminosity-weighted stellar dispersion within the  $3''$ -diameter SDSS aperture of  $\sigma_* \approx 270 \text{ km s}^{-1}$ , in good agreement with the observed value. Using the model to *de-lens* the four lensed images yields a source with a smooth, monotonically-decreasing brightness distribution. Taken in combination, the HST ACS images, Gemini IFU spectroscopy, and self-consistent mass model show SDSSJ1402 to be a genuine lens system.

*Subject headings:* Gravitational lensing—galaxies: elliptical and lenticular, cD—surveys

## 1. INTRODUCTION

In the last decade, galaxy-size gravitational lenses have become an increasingly important tool for the study of cosmology and galaxy evolution. The number of known lenses has now reached almost 100 (see the CASTLES web page at <http://cfa-www.harvard.edu/castles/>),

<sup>1</sup> Based on observations made with the NASA/ESA Hubble Space Telescope, obtained at the Space Telescope Science Institute, which is operated by the Association of Universities for Research in Astronomy, Inc., under NASA contract NAS 5-26555. These observations are associated with program #10174. Support for program #10174 was provided by NASA through a grant from the Space Telescope Science Institute, which is operated by the Association of Universities for Research in Astronomy, Inc., under NASA contract NAS 5-26555.

<sup>2</sup> Also based on observations obtained under program GN-2004A-Q-5 at the Gemini Observatory, which is operated by the Association of Universities for Research in Astronomy, Inc., under a cooperative agreement with the NSF on behalf of the Gemini partnership: the National Science Foundation (United States), the Particle Physics and Astronomy Research Council (United Kingdom), the National Research Council (Canada), CONICYT (Chile), the Australian Research Council (Australia), CNPq (Brazil) and CONICET (Argentina).

<sup>3</sup> Department of Physics and Center for Space Research, Massachusetts Institute of Technology, 77 Massachusetts Ave., Cambridge, MA 02139, USA ([bolton@mit.edu](mailto:bolton@mit.edu), [burles@mit.edu](mailto:burles@mit.edu))

<sup>4</sup> Kapteyn Institute, P.O. Box 800, 9700AV Groningen, The Netherlands ([koopmans@astro.rug.nl](mailto:koopmans@astro.rug.nl))

<sup>5</sup> Department of Physics and Astronomy, UCLA, Box 951547, Knudsen Hall, Los Angeles, CA 90095, USA ([ttreu@astro.ucla.edu](mailto:ttreu@astro.ucla.edu))

<sup>6</sup> Space Telescope Science Institute, 3700 San Martin Dr., Baltimore, MD 21218, USA ([leonidas@stsci.edu](mailto:leonidas@stsci.edu))

<sup>7</sup> Hubble Fellow

and subsets of lenses with suitable properties are now available for a variety of applications: the determination of the cosmological parameters from lens statistics (e.g. Turner et al. 1984; Kochanek 1996; Chae 2003), the measurement of the Hubble Constant from lens time delays (e.g. Kundić et al. 1997; Schechter et al. 1997; Koopmans et al. 2003), and the study of the mass distribution of E/S0 galaxies and their dark matter halos outside the local Universe (e.g. Kochanek 1994; Rusin et al. 2003; Treu & Koopmans 2004).

Despite the great progress, the small subsample sizes of suitable lenses is a major limitation. This is particularly true for the study of the properties of lens galaxies (typically E/S0s). Most currently known lenses have been discovered as bright quasars that show multiple images when observed at high spatial resolution. For optical quasar lenses, this biases the sample in favor of systems where the lensed source outshines the lens galaxy. Radio surveys such as the Cosmic Lens All-Sky Survey (CLASS; Myers et al. 2003; Browne et al. 2003) are less susceptible to this bias, but redshifts in radio lens systems can be difficult to obtain, and the lensing galaxies are often faint. This situation makes it very difficult to obtain high-quality photometry, redshifts, and internal kinematics of lens galaxies, which are essential ingredients for detailed modeling. It is not a coincidence that 3/5 lenses analyzed by the Lenses Structure and Dynamics Survey (LSD; Koopmans & Treu 2002, 2003; Treu & Koopmans 2002, 2003, 2004; hereafter collectively KT) so far have been discovered serendipitously in Hubble Space Telescope (HST) images.

To overcome this limitation we have initiated the Sloan Lens ACS (SLACS) Survey, a new survey for gravitational lenses that exploits the Sloan Digital Sky Survey (SDSS) archive and the angular resolution of HST to find and confirm new gravitational lenses. First, a large sample of SDSS early-type galaxy spectra is searched for emission lines at a higher redshift than that of the absorption features (Bolton et al. 2004; see also Warren et al. 1996). By requiring that the foreground galaxy dominate the absorption spectrum, this procedure will tend to select bright lenses with faint background sources. The second step consists of follow-up snapshot observations of the best candidates with the Advanced Camera for Survey (ACS) to confirm the incidence of lensing and provide the lens geometry necessary to construct a mass model<sup>8</sup>. Each candidate is observed for 420 seconds in each of F435W and F814W. The F435W filter is selected to optimize the detection of the lensed source galaxy (expected to be blue and starforming) while F814W is selected to optimize the signal-to-noise ratio on the (red) lens galaxy. Color information also provides important evidence in support of the lensing hypothesis. In this *Letter* we present the first newly discovered lens, along with ACS images and Gemini GMOS-North integral-field spectroscopy and a lens model, and discuss its overall properties. We assume that the Hubble constant, the matter density, and the cosmological constant are  $H_0 = 65 h_{65} \text{ km s}^{-1} \text{ Mpc}^{-1}$  (with  $h_{65} = 1$ ),  $\Omega_m = 0.3$ , and  $\Omega_\Lambda = 0.7$ , respectively. All spectroscopic wavelengths are given in vacuum values.

## 2. OBSERVATIONS

### 2.1. SDSS

The original spectroscopic observations of SDSSJ1402 were obtained on SDSS plate 605, fiber 503, MJD 52353 (included in the public Data Release 2). The latest public SDSS photometric values for the galaxy are  $(g, r, i) = (18.36, 17.00, 16.48)$ , all  $\pm 0.05$ , and it forms part of the volume-limited luminous red galaxy (LRG) spectroscopic sample (Eisenstein et al. 2001). The `specBS` one-dimensional spectroscopic pipeline (Schlegel et al., in preparation; see also Bolton et al. 2004) determines a redshift  $z = 0.2046 \pm 0.0001$  and a velocity dispersion of  $267 \pm 17 \text{ km s}^{-1}$  for SDSSJ1402. Though the spectrum is unambiguously that of an early-type galaxy at the above redshift, it also exhibits nebular line emission at a background redshift of  $0.4814 \pm 0.0001$  (see Figure 2 of Bolton et al. 2004). Given the measured stellar velocity dispersion and these redshifts and assuming a singular isothermal sphere galaxy model, one naively expects a strong-lensing region of radius  $2''.2 \pm 0''.3$  (twice the Einstein radius) in the plane of the sky, centered on the foreground galaxy. Considering the  $1''.5$  radius of an SDSS spectrograph fiber aperture, the prior probability of the system being a strong gravitational lens is essentially unity if one neglects the effects of seeing and fiber misalignment, and it was therefore targeted for follow-up observation.

<sup>8</sup> Our survey is the second HST snapshot lens survey. For details of the first, see Maoz et al. (1993).

### 2.2. HST-ACS

*Hubble Space Telescope* (HST) observations of SDSSJ1402 were obtained on 2004 August 4 with the Advanced Camera for Surveys (ACS), with one 420-second exposure in each of the filters F435W and F814W. The  $5\text{-}\sigma$  limits are approximately  $B_{435} \approx 22 \text{ mag arcsec}^{-2}$  and  $I_{814} \approx 23 \text{ mag arcsec}^{-2}$  in  $2 \times 2$ -pixel apertures. The brief exposure times result in cosmic rays affecting  $\sim 1\text{--}2\%$  of all pixels. These are very effectively flagged and cleaned using the Laplacian edge-detection technique (“LACOSMIC”) of van Dokkum (2001). The cosmo-c cleaned images are spatially transformed to an orthogonal coordinate system by the MULTIDRIZZLE routine as implemented on pyraf by STScI. This allows for high-precision astrometry and spatially-correct galaxy shapes. In each band, a 2D model of the lensing galaxy is computed using GALFIT (Peng et al. 2002). The fits are done assuming a simple Sérsic profile parametrized by index  $n$  (where  $n = 1$  is an exponential, and  $n = 4$  is a de Vaucouleur profile), as well as assuming a constrained de Vaucouleur profile. The latter is especially useful for comparison with fundamental plane results. The Sérsic fits are sufficiently accurate to produce high-quality residual images, which are used to measure the positions of candidate lensed images. These are identified both by their image configurations and by their similarity in  $B_{435} - I_{814}$  colors.

The constrained de Vaucouleur fit to the F814W galaxy image gives a model magnitude<sup>9</sup> of  $I_{814} = 16.28 \pm 0.01$ , an isophotal axis ratio  $q_{814} = 0.786 \pm 0.01$ , a position angle  $\theta_{814} = 71.0^\circ \pm 0.2^\circ$  East of North, and an intermediate-axis effective (half-light) radius of  $R_e = 2''.80 \pm 0''.01$ . Fixing the galaxy shape from these F814W de Vaucouleurs structural parameters and fitting for a magnitude in the F435 image yields  $B_{435} = 19.00 \pm 0.01$ . The unconstrained Sérsic fit to the F814W data has an index of  $n = 5.93 \pm 0.03$ , indicating a high degree of central concentration.

Figure 1 shows the ACS F435W and F814W images and galaxy-subtracted F435W residual image of SDSSJ1402. Despite low signal-to-noise, four images with similar colors are easily identifiable in both filters with a typical quad-like configuration; we designate these images A–D. Two of the images (A and B) appear arc-like in both filters and stretched tangentially. We determine image centroids from the F435W image, in which they are more pronounced and less affected by residuals from the foreground galaxy subtraction. Table 1 lists these image positions relative to the LRG centroid. We describe the determination of a gravitational-lens model based on these image positions in § 3 below.

### 2.3. Gemini GMOS-N IFU

To solidify the lensing hypothesis over alternative explanations for the observed features, we look to spatially resolved spectroscopy of SDSSJ1402 obtained with the integral-field unit (IFU) of the Gemini Multi-Object Spectrograph (GMOS-N) on the 8-meter Gemini North telescope at Mauna Kea (Hook et al. 2003; Allington-Smith et al. 2002). The observations were

<sup>9</sup> All HST magnitudes are corrected for dust extinction using Schlegel, Finkbeiner, & Davis (1998) maps.

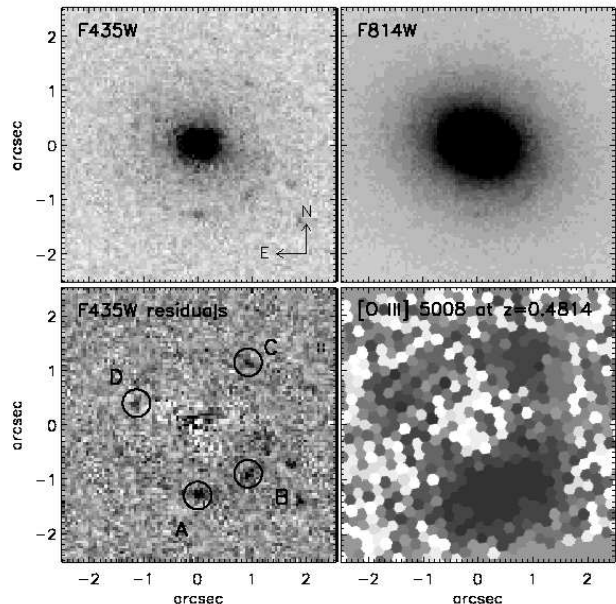


FIG. 1.— Imaging of SDSSJ1402. Top panels: ACS F435W (left) and ACS F814W (right) images. Lower left: ACS F435W galaxy-fit-subtracted residual image, with lensed image positions indicated. Lower right: reconstructed 5-Å-wide narrowband image from GMOS-N IFU spectroscopy, centered at a vacuum wavelength of 7420 Å corresponding to redshifted [OIII] 5008.24 Å. Note coincidence of line emission with lensed image positions. (IFU image scaling has been histogram-equalized.)

Image	$\Delta x$ (W)	$\Delta y$ (N)
A	+0'00	-1'35
B	+0'93	-0'95
C	+0'88	+1'15
D	-1'13	+0'45
G	$\equiv 0'00$	$\equiv 0'00$

TABLE 1  
ASTROMETRY OF THE LENSED IMAGES OF SDSSJ1402.

(Positions are determined by eye from the F435W residual image; we adopt conservative 0'.1 errors in right ascension and declination for the lens modeling described in § 3.)

made using the R600 grating and a Sloan *i*-band blocking filter to prevent spectral overlap and allow use of the full  $5'' \times 7''$  IFU field of view. The total integration time was  $3 \times 900$  seconds, and the data were reduced using custom IFU software written in IDL (Bolton & Burles, in preparation). In addition to the ACS data, Figure 1 also shows a reconstructed IFU narrow-band image of a 5-Å window about the redshifted [O III] 5008.24 Å emission, after subtraction of a linear fit to the LRG continuum at that wavelength. The emission is spatially coincident with the assumed lensed images in the HST-ACS data. Independent confirmation of the identification of this line emission as redshifted [OIII] is provided by summing the spectra in circular apertures about the approximate image positions to obtain the spectrum presented in Figure 2, showing both lines of the [OIII] doublet in the expected 1:3 ratio, as well as H $\beta$ . We thus confirm that the redshift of the faint images is much higher than that of the LRG, further

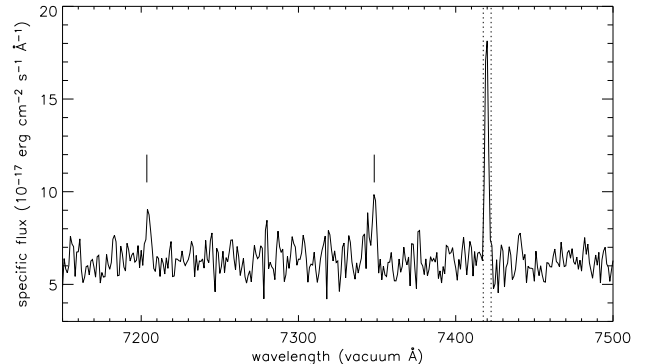


FIG. 2.— Summed GMOS-N IFU fiber spectra for fibers near the narrowband image positions seen in Figure 1 (without continuum subtraction). Redshifted H $\beta$  4863 Å and [OIII] 4960 Å are detected at the expected positions, as shown by tick marks above the spectrum. Dotted lines show the narrowband-image wavelength range used to generate the IFU image of Figure 1.

supporting a lensing interpretation.

### 3. GRAVITATIONAL-LENS MODEL

Adopting a lensing hypothesis for SDSSJ1402, we model the lens as a simple singular isothermal ellipsoidal (SIE) mass model without external shear, using the astrometry of the four images as constraints. Using the mass normalization from Kormann et al. (1994), the best-fit ( $\chi^2 = 2.1$  for NDF=3) gives an Einstein radius  $b = 1'35 \pm 0'05$  (68% CL), corresponding to a SIE velocity dispersion of  $\sigma_{\text{SIE}} = 292 \pm 6$  km/s<sup>10</sup> and a physical radius of  $(4.9 \pm 0.2)h_{65}^{-1}$  kpc. The axial ratio and position angle (in the frame of Figure 1) of the ellipsoidal equal surface density contours are  $q = 0.78^{+0.12}_{-0.11}$  and  $\theta = 63.6^{+2.2}_{-2.2}$  degrees, respectively. This lens-model ellipticity is in good agreement with the ellipticity of the galaxy isophotes given in § 2.2. The galaxy and lens-model position angles are also significantly aligned, although they differ formally by  $\approx 3\sigma$ .

The total mass-to-light ratio within the Einstein radius is robustly determined by the data, and we compute it as follows. The total mass enclosed by the critical curve is  $(30.9 \pm 2.3) \times 10^{10} h_{65}^{-1} M_{\odot}$ : we derive this from the fitted lens model, but it is in fact largely model independent. From aperture photometry, the corresponding enclosed magnitude is  $B_{435} = 20.28$ . Using a *specBS* template fitted to the spectrum of SDSSJ1402 and an ACS-F435W filter curve, we compute a *k*-correction of 1.20 for the lens galaxy. Combining this with a distance modulus of 40.17 from our assumed cosmology, we obtain an absolute  $B_{435}$  magnitude of  $-21.09 \pm 0.05$  enclosed by the lensed images, with an estimated 0.05-magnitude systematic error in the conversion. Finally, we convert from the *AB* system to Johnson *B* via  $B_{435} = B - 0.11$ , giving an absolute *B* magnitude of  $-20.98 \pm 0.05$ . For an absolute

<sup>10</sup> Recall that the luminosity-weighted stellar dispersion from the SDSS is  $\sigma_{\text{stloan}}^* = 267 \pm 17$  km/s (within a  $3''$  diameter aperture). Prior to the ACS observations we predicted  $b = 1'12 \pm 0'14$  based on this dispersion, leading to the selection as lens candidate.

solar magnitude of  $M_{B,\odot} = 5.47$  (Cox 2000), the rest-frame  $B$ -band luminosity within the Einstein radius is then  $L_{B,\text{encl}} = (3.8 \pm 0.2) \times 10^{10} h_{65}^{-2} L_{B,\odot}$ . Thus the enclosed  $B$ -band mass-to-light ratio is  $\Upsilon_B = (8.1 \pm 0.7) h_{65}$  in solar units.

If we assume the stars to be test particles embedded in an isothermal mass distribution with the above given mass, with a luminosity density derived from the stellar surface brightness (e.g. see KT03 or TK04 for details), we find a luminosity-weighted stellar dispersion of  $\sigma_*( < 3'') \approx 270 \text{ km s}^{-1}$  within the SDSS aperture, assuming an isotropic dispersion tensor. This agrees very well with the observed stellar dispersion. Future work will present a more detailed dynamical analysis based on the determination of an extended kinematic profile or field (e.g. with integral-field spectroscopy).

With this mass model, we proceed to *invert* the lensed images to obtain the structure of the source (e.g. Warren & Dye 2003; see also Treu & Koopmans 2004 for more details). We regularize the solution by adding a term to the penalty function that suppresses the curvature (see Press et al. 1992) of the resulting source brightness distribution. During the single-step inversion process the mass model remains fixed. We use PSF models generated with Tiny-Tim, although the results are insensitive to the precise PSF model because of the low S/N of the images. The F435W results are shown in Figure 3, for a regularization that gives  $\chi^2/\text{NDF} \approx 1.0$ . We see that the source has a roundish monotonically-decreasing brightness distribution, close to and inside the fold caustic. In the F814W filter (not shown), the source is found at the same position and with similar structure. Also shown are the lensed source model and residuals. The latter show no significant remaining structure and are distributed Gaussian. We find that models with parameters within the 68% CL of the best-fit SIE model values give similar results, but can not be distinguished at a significant level because of the low S/N of the images. Hence, the lens inversion should for now be regarded only as a consistency check of the lens model.

#### 4. CONCLUSIONS

Based on the following evidence, we conclude that SDSSJ1402 is a lens system:

1. The discovery of emission-lines in the SDSS spectrum at a redshift significantly larger than that of the high- $\sigma_*$  LRG and within a  $1.5''$  radius from the galaxy centroid, and confirmed by follow-up GMOS-N IFU spectroscopy.
2. The discovery of four images (with two tangentially stretched) in a typical quad-lens-like configuration around the galaxy in *Hubble Space Telescope* images, with similar colors and positions between F814W and F435W filters.
3. The spatial coincidence of these images with the higher-redshift line emission, as shown by GMOS-N IFU spectroscopy.
4. The excellent goodness-of-fit ( $\chi^2/\text{NDF} \approx 0.7$ ) for the SIE mass model (no external shear). The stellar velocity dispersion predicted by this mass model and the observed luminosity density is in excellent

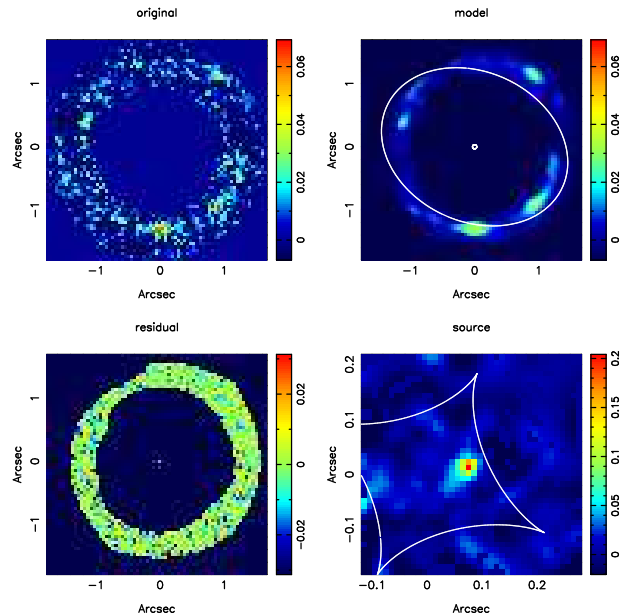


FIG. 3.— Gravitational-lens inversion of SDSSJ1402 in the F435W band. Upper left panel shows the galaxy-subtracted HST-ACS image within a suitable annulus. The best model of the system (upper right) is the mapping of the source model (lower right) on to the image plane using the best-fit SIE mass model. The critical curve and caustic are plotted on the image and source models, respectively. Data – model residual images are shown in the lower left panel.

agreement with the SDSS value, and the galaxy and lens-model ellipticities and position angles are in significant agreement with one another.

5. A direct inversion of the lensed image—based solely on the SIE mass model determined from the image positions—leads to a very simple compact source structure in both F814W and F435W filters at the same position near the inside of the fold caustic.

Hence, despite the relatively low signal-to-noise of the lensed images, the spectral and imaging data of SDSSJ1402 presented in this paper, in conjunction with the self-consistent lens model, convincingly show that the *first* candidate observed by the SLACS Survey is also the *first* genuine lens system from the program! The lens geometry and HST photometry yield a (largely model-independent) measurement of  $(30.9 \pm 2.3) \times 10^{10} h_{65}^{-1} M_{\odot}$  and a rest-frame  $B$ -band mass-to-light ratio of  $(8.1 \pm 0.7) h_{65}$  times solar within the  $(4.9 \pm 0.2) h_{65}^{-1}$ -kpc cylinder enclosed by the critical curve. Spatially resolved kinematic observations of this system will permit more detailed lens/dynamical modeling, which will constrain the radial mass profile and the relative fraction of luminous to dark matter in the central region of the lensing galaxy.

TT acknowledges support from NASA through Hubble Fellowship grant HF-011167.01.

L.A.M. acknowledges support from the Spitzer Legacy Science Program, provided by NASA through contract

1224666 issued by the Jet Propulsion Laboratory, California Institute of Technology, under NASA contract 1407.

The authors thank Hsiao-Wen Chen for the gracious provision of an ACS-F435W filter curve. We are grate-

ful for the scheduling work done by Galina Soutchkova, the Program Coordinator for this HST program (SNAP-10174).

#### REFERENCES

- Allington-Smith, J., et al. 2002, *PASP*, 114, 892  
 Bolton, A. S., Burles, S., Schlegel, D. J., Eisenstein, D. J., & Brinkmann, J. 2004, *AJ*, 127, 1860  
 Browne, I. W. A., et al. 2003, *MNRAS*, 341, 13  
 Chae, K. 2003, *MNRAS*, 346, 746  
 Cox, A. N. 2000, *Allen's astrophysical quantities* (Allen's astrophysical quantities, 4th ed. Publisher: New York: AIP Press; Springer, 2000. Edited by Arthur N. Cox. ISBN: 0387987460)  
 Eisenstein, D. J., et al. 2001, *AJ*, 122, 2267  
 Hook, I., et al. 2003, in *Instrument Design and Performance for Optical/Infrared Ground-based Telescopes*. Edited by Iye, Masanori; Moorwood, Alan F. M. *Proceedings of the SPIE*, Volume 4841, pp. 1645-1656 (2003)., 1645-1656  
 Kochanek, C. S. 1994, *ApJ*, 436, 56  
 —. 1996, *ApJ*, 466, 638  
 Koopmans, L. V. E., & Treu, T. 2002, *ApJ*, 568, L5  
 —. 2003, *ApJ*, 583, 606  
 Koopmans, L. V. E., Treu, T., Fassnacht, C. D., Blandford, R. D., & Surpi, G. 2003, *ApJ*, 599, 70  
 Kormann, R., Schneider, P., & Bartelmann, M. 1994, *A&A*, 284, 285  
 Kundić, T., et al. 1997, *ApJ*, 482, 75  
 Maoz, D., et al. 1993, *ApJ*, 409, 28  
 Myers, S. T., et al. 2003, *MNRAS*, 341, 1  
 Peng, C. Y., Ho, L. C., Impey, C. D., & Rix, H. 2002, *AJ*, 124, 266  
 Rusin, D., Kochanek, C. S., & Keeton, C. R. 2003, *ApJ*, 595, 29  
 Schechter, P. L., et al. 1997, *ApJ*, 475, L85+  
 Schlegel, D. J., Finkbeiner, D. P., & Davis, M. 1998, *ApJ*, 500, 525  
 Treu, T., & Koopmans, L. V. E. 2002, *ApJ*, 575, 87  
 —. 2003, *MNRAS*, 343, L29  
 —. 2004, *ApJ*, 611, 739  
 Turner, E. L., Ostriker, J. P., & Gott, J. R. 1984, *ApJ*, 284, 1  
 van Dokkum, P. G. 2001, *PASP*, 113, 1420  
 Warren, S. J., & Dye, S. 2003, *ApJ*, 590, 673  
 Warren, S. J., Hewett, P. C., Lewis, G. F., Moller, P., Iovino, A., & Shaver, P. A. 1996, *MNRAS*, 278, 139